

## Review



**Cite this article:** Iqbal S, Xu Y, Boyd RW. 2024 Limitations in quantum metrology approaches to imaging resolution. *Phil. Trans. R. Soc. A* **382**: 20230332.

<https://doi.org/10.1098/rsta.2023.0332>

Received: 27 May 2024

Accepted: 14 August 2024

One contribution of 18 to a theme issue 'The quantum theory of light'.

**Subject Areas:**

quantum engineering, quantum physics, optics, light microscopy

**Keywords:**

quantum optics, quantum metrology, quantum imaging, super-resolution, localization

**Author for correspondence:**

S. Iqbal

e-mail: [siqbal3@ur.rochester.edu](mailto:siqbal3@ur.rochester.edu)

Limitations in quantum  
metrology approaches to  
imaging resolution

S. Iqbal<sup>1</sup>, Y. Xu<sup>2</sup> and R. W. Boyd<sup>1,3</sup>

<sup>1</sup>Institute of Optics, University of Rochester, Rochester, NY 14627, USA

<sup>2</sup>Department of Physics and Astronomy, University of Rochester, Rochester, NY 14627, USA

<sup>3</sup>Department of Physics, University of Ottawa, Ottawa, Ontario K1N 6N5, Canada

SI, 0009-0009-8503-7841; RWB, 0009-0009-8503-7841

Can a quantum advantage for imaging resolution be realized with the help of quantum estimation theory? We expect so, but we show that, presently, theoretical tools are insufficiently developed to answer this question for extended objects. Still, there is much to be learned from the current state of the art. In this review, we re-examine prominent results in the literature and probe the limits of quantum metrology in addressing imaging resolution. In particular, we show that under restrictive but well-defined conditions, any quantum advantage in one-dimensional phase imaging appears to diminish for increasingly detailed objects. We also show that a previous attempt at tackling this question, while incomplete, does predict an advantage for single-molecule localization microscopy, although this method may not be feasible in the near term. As for experimental claims of Heisenberg-limited imaging resolution, we briefly address the many inherent difficulties in demonstrating that such a thing has indeed been achieved.

This article is part of the theme issue 'The quantum theory of light'.

## 1. Introduction

The recent successes of quantum metrology in the interferometric detection of gravitational waves [1] and in coherent Raman microscopy of living cells [2] naturally prompt the question of whether estimation

approaches to other problems might yield concrete benefits. Largely due to its potential for applications in biology [3], astronomy [4], and lithography [5], among other important areas, the possibility of a metrological quantum advantage for imaging resolution has been a long-pursued and frequently debated goal.

Here, we critically review some of the prominent existing work on this subject, with our ultimate conclusion being that in its current form, quantum estimation theory, is insufficiently developed for us to establish with complete confidence the existence of such an advantage.

This statement may surprise some researchers who are active in this field, due to several theoretical and experimental works [6–8] that claim otherwise. To resolve these discrepancies, we first turn to the treatment of imaging as an estimation problem and discuss why imaging is not a problem of parameter estimation but of function estimation. Using an existing treatment [9] of quantum estimation of uniformly continuous, one-dimensional phase functions, we show why one might expect that any quantum advantage in reconstructing a pure phase object is degraded for samples with increasingly fine details. In fact, for the most intricately detailed objects, the advantage may be entirely negligible.

We then return to the claims of some existing works and show that by attempting to reduce imaging resolution to a single-parameter estimation problem, one naturally constrains the types of objects and the information about these objects that such a theory applies to. This, of course, does not mean that single-parameter approaches are useless, but that they are best applied to answering specific questions about specific classes of objects, rather than as a viable tool for super-resolution imaging of arbitrary objects. As an example, we show that a previous attempt at establishing a metrological quantum advantage for imaging resolution can only currently be proven to apply to point-source localization. This capability leads naturally to a quantum-enhanced version of single-molecule localization microscopy (SMLM) [10], which can likely achieve super-resolved precision with lower photon fluxes than what can be done classically. However, as we show below, a near-term implementation of this modality seems unlikely.

We next discuss why experimental demonstrations of resolution enhancement in a quantum imaging system do not rule out the possibility of a classical imaging system closely (or entirely) replicating its performance. As a result, experimental studies that claim to achieve a Heisenberg limit (HL) for imaging resolution suffer from having been misled by single-parameter estimation approaches that do not apply to their specific imaging systems and problems. We emphasize that just because it may be possible to reproduce some of these enhancements classically, this does not mean these results have no utility. Quantum imaging systems that offer capabilities that are not currently available for classical systems have obvious benefits in the near term and may inspire the development of classical techniques with superior or complementary features in the future.

## 2. Imaging is not generally a parameter estimation problem

Researchers having some familiarity with quantum metrology [11,12] are likely acquainted with the single-parameter standard quantum limit (SQL) and HL for the root-mean-square error (RMSE) in the unbiased estimation of a given parameter, namely

$$\sigma_{\text{SQL}} \propto \frac{1}{\sqrt{mN}} \quad (2.1)$$

$$\sigma_{\text{HL}} \propto \frac{1}{\sqrt{mN'}} \quad (2.2)$$

where  $N$  is the number of probes (in this case, photons) and  $m$  is the number of independent  $N$ -photon wave packets used to probe the sample. Another intuitive way of thinking about  $m$  is that it is the number of ‘rounds’ in which the sample is interrogated by the  $N$  photons. These

equations give the well-known scaling advantage in employing an  $N$ -photon quantum state in estimating a single parameter (the HL scenario) over using the  $N$ -th order correlations of classical light (the SQL scenario) of

$$\frac{\sigma_{\text{HL}}}{\sigma_{\text{SQL}}} \propto \frac{1}{\sqrt{N}}. \quad (2.3)$$

It is important to note that this is not a general result. The conventional formulation of the HL requires assumptions about the nature of the interaction between the probes and the sample under study, and about the evolution of the probes immediately after that interaction until a measurement is performed. In particular, each of the probes is assumed to be independently affected by the sample [13] and the evolution of the probes thereafter until they are detected is assumed to be linear and free of decoherence [14]. We will revisit these assumptions and their implications for imaging below.

As we mentioned, imaging is not generally a parameter estimation problem. In general, by performing imaging, we wish to reconstruct an unknown two-dimensional function that contains information about a sample. Examples of such a function include the variation in the amplitude, phase, or retardance associated with the sample transmittance as a function of the lateral spatial coordinates. Three-dimensional imaging is also of interest, but in some sense is largely a separate topic. Unfortunately, a quantum theory of two-dimensional function estimation does not yet exist. The next best option is provided in a recent work by Kura & Ueda [9] in which they derived an SQL and HL for the estimation of a one-dimensional, uniformly continuous phase function. Note that the authors did not include the effects of multiple rounds of interrogation.

This study [9] is, however, limited in its ability to faithfully model phase imaging, as it neglects the inherent attenuation of sufficiently high spatial-frequency components of the field by either the finite aperture of the imaging optics or evanescent decay in the near-field of the sample [15]. It also requires that the object lie entirely within the field of view of the optical system. Note that these issues also occur in works that use the estimation of a discrete set of multiple phases [16,17] as a model for phase imaging.

If we narrow the scope of our questions accordingly, we can use the results of [9] to obtain an SQL and HL for one-dimensional quantitative phase imaging restricted to a single round of interrogation ( $m = 1$ ), and limited to objects that are easily resolved and lie entirely within the field of view. Kura and Ueda find that the quantum advantage in employing an  $N$ -photon quantum state scales with photon number as

$$\frac{\sigma_{\text{HL}}}{\sigma_{\text{SQL}}} \propto N^{-q^2/(2q^2+3q+1)}, \quad (2.4)$$

where  $q$  is a parameter specifying the smoothness of the phase object, and the associated MSEs have been averaged over its transverse spatial extent. The smoothness parameter  $q$  is defined such that the magnitude of the coefficients of the Fourier series representation  $|\phi_k|$  of the phase object must decay faster than  $k^{-q}$  as  $k \rightarrow \infty$ . The domain of  $q$  is  $q > 0$  with the limit as  $q \rightarrow 0$  corresponding to an object that is not uniformly continuous (and possibly discontinuous) and the limit as  $q \rightarrow \infty$  corresponding to an object with no spatial dependence (i.e. it is constant). Both of these asymptotic limits are worth examining.

As can be verified using equation (2.4), the latter recovers the result of single-parameter estimation given by equation (2.3), as it should. The former, however, yields

$$\lim_{q \rightarrow 0} \frac{\sigma_{\text{HL}}}{\sigma_{\text{SQL}}} \propto N^0 = 1, \quad (2.5)$$

which is a much more surprising result. In the language of imaging,  $q$  is a measure of the finest level of detail in a specified object, as it suppresses the contribution of high spatial-frequency components to the phase object  $\phi(x)$ . Smaller values of  $q$  indicate the presence of sharper

features in the sample, while larger values indicate their absence. Equation (2.5) tells us that as the level of detail in the object gets finer and finer, any quantum advantage in estimating it becomes independent of photon number. This behaviour is demonstrated in figure 1, where the right-hand side of equation (2.4) is plotted for several values of  $N$ . Note that in the asymptotic limit represented in equation (2.5), it may be valid to replace the proportionality with an equality, indicating that any quantum advantage in estimating the object has entirely disappeared. For further details, we refer the interested reader to equations (5) and (6) in [9].

Essentially, this result implies that as we attempt to image samples in increasing detail, we might expect any metrological advantage gained through the use of  $N$ -photon quantum states to diminish accordingly. A generalization of this result to treat objects that cannot be easily resolved by the imaging system is likely needed to ensure the universality of this conclusion, but we should keep it in mind nonetheless, as it demonstrates that naive extrapolations of results from single-parameter estimation to more complicated scenarios are limited in what they can tell us. Note, however, that this still does mean that we can expect there to be substantial advantages for the imaging of phase objects with a low or intermediate level of detail.

We should also note that the scenario presented here is somewhat artificial, as quantum imaging typically involves image formation from a large number ( $m \gg 1$ ) of independent  $N$ -photon wave packets with  $N$  typically being quite small (and often just 2 or 3). Accordingly, a generalization of the results of [9], which includes the effect of multiple rounds of interrogation, would also be desirable.

### 3. The difference between localization and imaging

We now turn to claims of an SQL and HL for imaging resolution that are based on single-parameter estimation theory. In particular, the work of Giovannetti *et al.* [6] may be the most significant and representative of this approach. The authors suggest the existence of a general quantum advantage for imaging resolution that can be achieved using Fock state illumination and  $N$ -photon detection. In what follows, we show that their results instead only imply that for  $N > 1$ , a Fock state point source can be localized more precisely than a classical point source. For readers lacking a substantial background in imaging, note that within two-dimensional and paraxial treatments (such as that of [6]), the term ‘point source’ is frequently used to refer to an object with a spatial extent small enough so as to be indistinguishable from (either a primary or secondary) point source of electromagnetic radiation located in the focal plane of the imaging system.

While this restriction limits the breadth of imaging scenarios in which their results are applicable, it also establishes a quantum advantage for an existing class of super-resolution techniques known as SMLM [10], two popular variants of which are stochastic optical reconstruction microscopy and photoactivated localization microscopy.

The relevant imaging schemes discussed by Giovannetti *et al.* were stated to be governed by resolution limits they refer to as the coherent and incoherent SQL (equations (3.1) and (3.2), respectively) and the coherent and incoherent HL (equations (3.3) and (3.4), respectively). The point-spread functions (PSFs) they derived for each case are given below:

$$h_{\text{CSQL}}(\vec{r}) = h^N(\vec{r}), \quad (3.1)$$

$$h_{\text{ISQL}}(\vec{r}) = |h(\vec{r})|^{2N}, \quad (3.2)$$

$$h_{\text{CHL}}(\vec{r}) = h(N\vec{r}), \quad (3.3)$$

$$h_{\text{IHL}}(\vec{r}) = |h(N\vec{r})|^2, \quad (3.4)$$

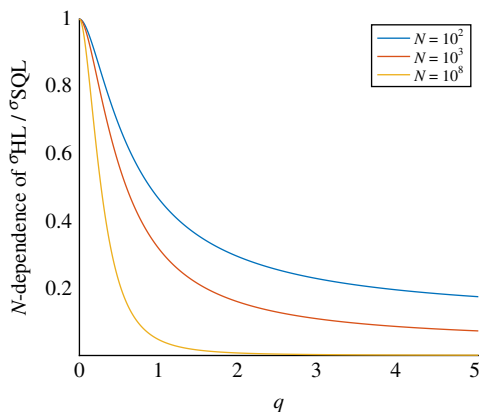


**Figure 1.** Photon-number scaling of the expected quantum advantage in one-dimensional quantitative phase imaging restricted to the detection of a single  $N$ -photon wave packet ( $m = 1$ ), as written in the right-hand side of equation (2.4). The parameter  $q$  describes the finest level of detail present in the object, with smaller values indicating that it possesses sharper features. The chosen photon numbers correspond to low and high light levels for typical imaging situations [18], along with an intermediary value. Clearly, any appreciable quantum advantage in the precision of the estimation gained through the use of  $N$ -photon quantum states vanishes for finely detailed objects.

where  $h(\vec{r})$  is the classical coherent PSF. Note that the terms ‘coherent’ and ‘incoherent’ here refer to whether the object is illuminated with a coherent superposition or incoherent mixture of  $N$ -photon Fock states. Note also that the only difference between the imaging system leading to equations (3.1) and (3.2) and the one leading to equations (3.3) and (3.4) is the presence of a photon-number-discriminating screen immediately in front of the imaging objective, a difference we revisit below. Equation (3.2), the PSF said to be governed by an incoherent SQL, is also the PSF for existing classical SMLM techniques in the absence of noise and the localization precision of these techniques is also given by equation (2.1).

For the sake of illustration, the PSFs associated with what were termed the incoherent SQL and HL are plotted for different values of  $N$  in figure 2. Recall that the numerical aperture of the objective is defined as  $NA = n \sin \alpha$ , where  $n$  is the refractive index of the medium between the object plane and the objective and  $\alpha$  is the on-axis half-angle subtended by the objective entrance pupil at the object plane.

To determine the photon-number scaling of equations (3.1)–(3.4), the authors determined the radius at which the area under each PSF is 84% of the total over its entire domain. From an estimation perspective, this is not the primary quantity of interest. Instead, we should treat each PSF as a probability density function that describes the error in unbiased estimation of the location of a point source in the object plane. Then, we can compute the RMSEs associated with each and determine their photon-number dependence.

Before proceeding, it is important to note that a probability distribution must be non-negative for all values of its argument. This means that  $h_{\text{CSQL}}(\vec{r})$  and  $h_{\text{CHL}}(\vec{r})$  cannot themselves be probability distributions, although their squared magnitudes can be, so that a single treatment suffices for direct imaging in both the coherent and incoherent cases. This of course only makes sense, as a point source must be coherent with itself.

If one treats the realistic situation of an imaging system with an unapodized circular pupil, the integrals involved with computing the RMSE do not yield a closed-form expression. In the theory underpinning SMLM, a commonly used simplification is the approximation of the Airy pattern corresponding to  $|h(\vec{r})|^2$  by a Gaussian distribution of equal volume (to preserve normalization), an approximation we also make here.

Also worth noting is that two-dimensional point-source localization is intrinsically a two-parameter estimation problem, the two parameters of course being the lateral spatial

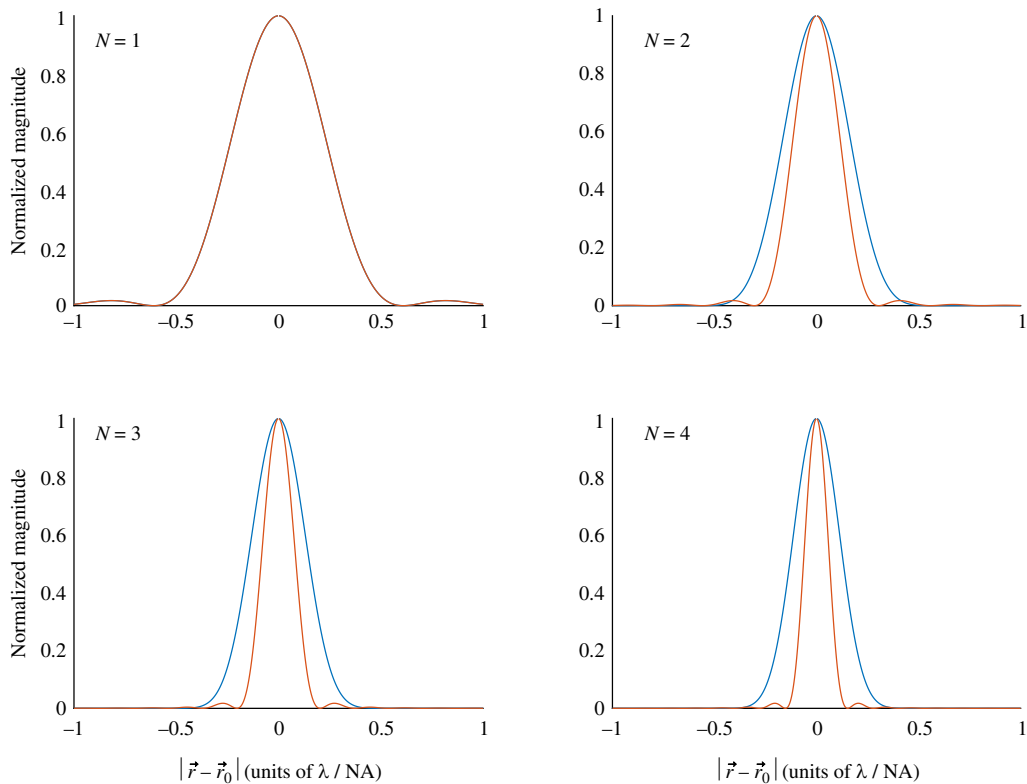


**Figure 2.** PSFs associated with the SQL for classical point-source localization (blue) and the Heisenberg-like precision achievable for quantum point-source localization (orange), demonstrating the advantageous scaling with increasing photon number. Note that for  $N = 1$ , the two curves lie exactly on top of one another, and that  $\lambda$  is the wavelength of the light.

coordinates of the point source in the object plane. However, we can reduce this to two independent single-parameter problems that can be solved sequentially without any loss of generality. This is because the blurring actions along the two lateral dimensions (resulting from the convolution of the object with each PSF) are uncorrelated, i.e. the covariance between  $x$  and  $y$  is zero.

With these specifications accounted for, we now proceed with the calculation. The classical incoherent PSF  $|h(\vec{r})|^2$  of a widefield two-dimensional imaging system can be approximated with high accuracy by a Gaussian distribution

$$|h(\vec{r})|^2 \approx e^{-\frac{r^2}{2\sigma_{\text{PSF}}^2}}, \quad (3.5)$$

where  $\sigma_{\text{PSF}}$  is given by equation (11) in [19]. Note that this approximation is valid for scalar, non-paraxial imaging and is therefore accurate at high numerical apertures as long as vectorial effects play no significant role.

To show that directly imaging a Fock state point source with a photon-number-resolving (PNR) image sensor achieves SQL-like precision for two-dimensional point-source localization, we can use equations (3.2) and (3.5) to compute the image of a point source located at a lateral position  $\vec{r}_0$  (ignoring magnification for simplicity) in the object plane

$$I_{\text{SQL}}(\vec{r} - \vec{r}_0) = \frac{N}{\pi\sigma_{\text{PSF}}^2} e^{-2N \left[ \frac{(x-x_0)^2 + (y-y_0)^2}{2\sigma_{\text{PSF}}^2} \right]}, \quad (3.6)$$

in which we have introduced a prefactor to ensure normalization. Treating equation (3.6) as a probability distribution, we now see that our supposition that this estimation problem can be



treated sequentially as two independent single-parameter problems was a good one. Clearly,  $I_{\text{SQL}}(\vec{r} - \vec{r}_0)$  is separable in  $x$  and  $y$ .

For the estimation to be unbiased, we must assume that the estimation strategy (e.g. maximum likelihood estimation using data captured directly by an image sensor) introduces negligible additional errors. At the expense of the field of view, this requirement can be met by ensuring that the magnification of our imaging system along with the pixel pitch and fill factor of the image sensor are such that the Nyquist–Shannon sampling theorem is satisfied (i.e. no image pixelation occurs).

Assuming that this is so, the RMSE in estimation along both  $x$  and  $y$  is simply given by the variance of  $I_{\text{SQL}}(\vec{r} - \vec{r}_0)$ . As [equation \(3.6\)](#) is again a Gaussian distribution, this yields

$$\sigma_{\text{SQL}} = \frac{\sigma_{\text{PSF}}}{\sqrt{2N}}, \quad (3.7)$$

which clearly satisfies the proportionality in [equation \(2.1\)](#). This explicitly proves that the precision with which a Fock state point source can be localized by directly imaging it with a PNR image sensor is identical to that associated with the Cramér–Rao bound for classical two-dimensional point-source localization, which was established with full generality in [20]. Note that this does not immediately provide any new experimental capabilities, as conventional SMLM also achieves this precision (at least in the absence of noise, which we have also neglected in our treatment).

Now let us proceed to the scenario that has been proposed for realizing a Heisenberg-like scaling for imaging resolution. Giovanetti *et al.* [6] suggest the use of a two-dimensional photon-number-discriminating screen, which would be placed immediately in front of the imaging objective. Their derivation is only briefly sketched, so it is worth making the action of the screen more explicit here. In our derivation, the screen is placed in the back focal plane of the objective, but we expect that this difference with the treatment in [6] is immaterial. This screen would coherently transmit  $N$ -photon wave packets if all  $N$  photons strike the same location on the screen and completely reject the wave packet otherwise. We stress that such a screen has never been demonstrated experimentally nor do we believe that it would be easy to do so, although several works have suggested that it can, in principle, be constructed (see, for example, [21], and references therein).

With the near-term feasibility of this approach momentarily sidelined, recall that by assumption the light radiated by the point source is in an  $N$ -photon Fock state. Written in the continuous mode representation, this state is

$$|\Psi\rangle = |N; \vec{r}_0\rangle = \left[ \hat{a}^\dagger(\vec{r}_0) \right]^N |0\rangle, \quad (3.8)$$

where again  $\vec{r}_0$  specifies the lateral position of the point source in the object plane. As the creation operator  $\hat{a}^\dagger(\vec{r}, z)$  is a solution to the paraxial Helmholtz equation (see, for example, [equation \(3.27\)](#) of [22]), its evolution in the Heisenberg picture is the same as the propagation of a classical coherent field. This means that we may write the creation operator in [equation \(3.8\)](#) as [15]

$$\hat{a}^\dagger(\vec{r}_0) \propto \int d\vec{r}_1 H\left(\frac{\vec{r}_1}{\lambda f}\right) \hat{a}^\dagger(\vec{r}_1) e^{i\frac{2\pi}{\lambda f} \vec{r}_0 \cdot \vec{r}_1}, \quad (3.9)$$

where  $f$  is the effective focal length of the objective,  $\vec{r}_1$  specifies the lateral spatial coordinates in its back focal plane, and  $H(\vec{r}_1/\lambda f)$  is the coherent transfer function dictated by its finite aperture. Note that throughout this derivation, we drop constants of proportionality and simply ensure normalization in the final result. Inserting this expression into [equation \(3.8\)](#) yields

$$|\Psi\rangle = \int \left[ \prod_{m=1}^N d\vec{r}_m H\left(\frac{\vec{r}_m}{\lambda f}\right) \right] e^{i\frac{2\pi}{\lambda f} \sum_{m=1}^N \vec{r}_m \cdot \vec{r}_0} |1; \vec{r}_1, \dots, 1; \vec{r}_N\rangle. \quad (3.10)$$

The action of the photon-number-discriminating screen located in the objective back focal plane can then be expressed as a projection defined by the operator

$$\hat{P}_N = \int d\vec{r}_p |N:\vec{r}_p\rangle\langle N:\vec{r}_p|, \quad (3.11)$$

where we have assumed that the transverse dimensions of the screen are larger than the spatial extent of the field so that the integration bounds can be extended to infinity. This results in the projected state

$$|\Psi_P\rangle = \hat{P}_N|\Psi\rangle = \int d\vec{r}_p H\left(\frac{\vec{r}_p}{\lambda f}\right) e^{i\frac{2\pi N}{\lambda f}\vec{r}_p \cdot \vec{r}_0} |N:\vec{r}_p\rangle, \quad (3.12)$$

where we have used the fact that  $H^N(\vec{r}/\lambda f) = H(\vec{r}/\lambda f)$  for a well-corrected (i.e. practically aberration-free) imaging system [15]. We can now write the state of the field in the image plane using the fact that

$$\hat{a}^+(\vec{r}_p) \propto \int d\vec{r}_{1i} \hat{a}^+(\vec{r}_{1i}) e^{-i\frac{2\pi}{\lambda f}\vec{r}_p \cdot \vec{r}_{1i}}, \quad (3.13)$$

where  $\vec{r}_{1i}$  specifies the lateral spatial coordinates in the image plane, and we have assumed that the tube lens is a negative lens with the same effective focal length as the objective. Note that this assumption is not required, and is merely used to ensure that the image is uninverted and that the system possesses unit magnification for simplicity [15]. Inserting this expression into equation (3.12) yields

$$|\Psi_P\rangle = \int d\vec{r}_p H\left(\frac{\vec{r}_p}{\lambda f}\right) e^{i\frac{2\pi N}{\lambda f}\vec{r}_p \cdot \vec{r}_0} \int \left(\prod_{m=1}^N d\vec{r}_{mi}\right) e^{-i\frac{2\pi}{\lambda f}\sum_{m=1}^N \vec{r}_{mi} \cdot \vec{r}_p} |1:\vec{r}_{1i}, \dots, 1:\vec{r}_{Ni}\rangle \quad (3.14)$$

so that we can now compute the  $N$ -photon detection probability as

$$\begin{aligned} I_{\text{HL}}(\vec{r} - \vec{r}_0) &= \langle [\hat{E}^+(\vec{r})]^N [\hat{E}(\vec{r})]^N \rangle \\ &= \iint d\vec{r}_p d\vec{r}_{p1} H\left(\frac{\vec{r}_p}{\lambda f}\right) H^*\left(\frac{\vec{r}_{p1}}{\lambda f}\right) e^{i\frac{2\pi N}{\lambda f}(\vec{r}_{p1} - \vec{r}_p) \cdot (\vec{r} - \vec{r}_0)} \end{aligned} \quad (3.15)$$

which is very nearly the desired result. Two final steps remain. First, let us make the substitution  $\vec{r}_{p1} = \vec{r}_{p0} - \vec{r}_p$  and use the fact that  $H^*(\vec{r}_{p1}/\lambda f) = H^*(-\vec{r}_{p1}/\lambda f)$  for a well-corrected imaging system [15]. This procedure yields

$$I_{\text{HL}}(\vec{r} - \vec{r}_0) = \int d\vec{r}_{p0} \left[ \int d\vec{r}_p H\left(\frac{\vec{r}_p}{\lambda f}\right) H^*\left(\frac{\vec{r}_p - \vec{r}_{p0}}{\lambda f}\right) \right] e^{i\frac{2\pi N}{\lambda f}(\vec{r} - \vec{r}_0) \cdot \vec{r}_{p0}}, \quad (3.16)$$

where the inner integral (within the square brackets) should be recognized as an autocorrelation and the outer integral as an inverse Fourier transform. A straightforward application of the autocorrelation theorem then yields our final result [15]

$$I_{\text{HL}}(\vec{r} - \vec{r}_0) = |h[N(\vec{r} - \vec{r}_0)]|^2, \quad (3.17)$$

which is the same expression as equation (3.4). We may now make use of equation (3.17) and equation (3.5) to compute the image of this point source, namely

$$I_{\text{HL}}(\vec{r} - \vec{r}_0) = \frac{N^2}{2\pi\sigma_{\text{PSF}}^2} e^{-N^2 \left[ \frac{(x-x_0)^2 + (y-y_0)^2}{2\sigma_{\text{PSF}}^2} \right]}, \quad (3.18)$$

for which we have again normalized the result. With the same assumptions in place to guarantee an unbiased estimation, the RMSE is then



$$\sigma_{\text{HL}} = \frac{\sigma_{\text{PSF}}}{N}, \quad (3.19)$$

which satisfies the proportionality of equation (2.2). This seemingly indicates that direct imaging of the discriminated Fock state point source with a PNR image sensor achieves an HL for two-dimensional point-source localization. However, now we must revisit the limited generality of the HL. As we mentioned above, the cause of limited spatial resolution in an imaging system is the partial or complete loss of sufficiently off-axis plane-wave components of the field. The losses inherent to the problem of imaging resolution imply that conventional formulations of the HL, which rely on the decoherence-free evolution of the field prior to its detection [14], may not be applicable at all. So we will exercise caution and simply refer to this as quantum-enhanced point-source localization.

Let us assess exactly what has been demonstrated thus far. We have shown that there is a quantum advantage for estimating the location of a single point source in the object plane. Under what conditions can we generalize this result to the imaging of an extended two-dimensional object? This is precisely where treatments such as that of [6] are unclear, yet it appears that many researchers have assumed that this generalization is implicit in the form of equations (3.1)–(3.4) anyway. Luckily, we need not reinvent a solution, as microscopists solved this problem long ago for SMLM. The appropriate condition is a sparsity constraint, namely that the object can be safely approximated as a collection of isolated point sources. In practice, this means that the PSFs associated with each point source must be non-overlapping for each recorded image, as otherwise, it would be impossible to unambiguously identify the number of point-like objects in the scene. This principle is illustrated in figure 3. Unfortunately, most objects of interest violate this sparsity constraint in spectacular fashion.

In SMLM, this issue is addressed by exciting only a subset of fluorophores during the exposure time for a single frame and then performing post-processing on the results of many frames to reconstruct a super-resolved image. The accompanying increase in the number of frames required to form a single image means that SMLM is typically too slow to be compatible with the imaging of dynamically evolving processes. One can imagine that incorporating Fock state sources, the hypothetical photon-number-discriminating screen, and  $N$ -photon detection into SMLM may prolong image acquisition times beyond the point of utility for most applications.

Also, while (inefficient) PNR image sensors already exist and are commercially available [23], Fock state sources are much less well-developed [24,25]. Moreover, if we wish to localize primary point sources that the object has been labelled with, this would require fluorophores that emit light in a Fock state of definite photon number, which (to the best of our knowledge) have not been realized for  $N > 1$ .

While difficult to achieve, the quantum-enhanced localization resulting from the proposal in [6] likely allows one to achieve the same precision that classical SMLM techniques can, but having illuminated the object with less intense light. This capability would certainly be of use in applications suffering from photobleaching or photodamage. As we have just mentioned though, this modality is largely predicated on the use of Fock state fluorophores and a photon-number-discriminating screen, which do not yet exist, so we do not expect that quantum-enhanced SMLM can be realized in the near future.

## 4. How useful are spatial mode decomposition approaches?

One well-known use of quantum metrology in imaging applications is a technique for estimating the separation between pairs of mutually incoherent point sources known as spatial mode demultiplexing (SPADE) [26,27]. This technique is, of course, inspired by the Rayleigh two-point resolution criterion. While successful in solving the specific problem it was formulated to address, SPADE has encountered difficulties in its generalization to scenarios that might

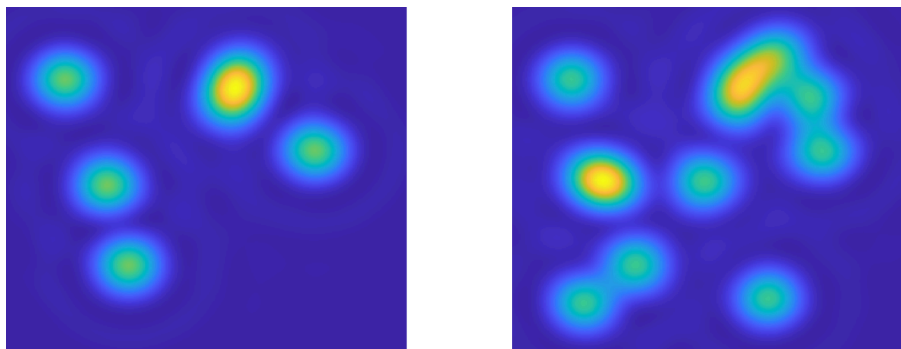


**Figure 3.** Simulated classical incoherent images of 6 (left) and 12 (right) equal-amplitude point sources. Note the difficulty in distinguishing the presence of multiple faint, overlapping sources from the presence of one brighter one.

enable a broader scope of applications. The main desirable generalizations would be to (i) extended two- or three-dimensional objects and (ii) fully and partially coherent imaging.

In the first case, our comments in the previous section regarding the approximation of an extended object as a collection of point sources likely still apply. For the time being, we therefore expect that the advantages conferred by SPADE-like approaches will be limited to extended objects that are sufficiently sparse so as to guarantee that the PSFs associated with different points are non-overlapping. As with SMLM [10], this requirement can be enforced by sequentially illuminating only a small portion of the object for each round of demultiplexing and then reconstructing a final image afterwards. This, of course, comes at the expense of imaging speed.

In the second case, it is important to note that two-point resolution criteria are object-dependent measures of spatial resolution in coherent [28] and partially coherent (see subsection 7.5.1 of [29]) imaging systems. It is also prudent to recall that spatially incoherent illumination is a limiting case of partial coherence that cannot be realized when employing high-resolution imaging optics (see subsection 7.4.3 of [29]).

Taken together, these considerations imply that SPADE may only be of immediate utility in the imaging of self-luminous or astronomical objects. The significance of the former is lessened by the existence of several techniques for super-resolution fluorescence microscopy [30–32], but the latter may present an opportunity for SPADE to make a near-term impact.

A suitable example along these lines is the problem of detecting an exoplanet in proximity to a much brighter star. SPADE-like approaches that coherently reject the field in the image plane associated with the star while retaining all other Zernike modes have been shown to be optimal for detecting the presence of the exoplanet [33]. However, it is important to note that this solution is not very different from the traditional approach to coronagraphy (see section 8.3 of [15]), which typically involves the partial rejection of the light coming from the star, and it also does not seem to make use of any nonclassical effects. Perhaps the truly novel aspect is the development of a new classical method for more elegantly implementing an intuitive solution. Note that the necessary Zernike mode sorter for implementing the optimal solution of [33] has only recently been demonstrated experimentally [34].

The issue regarding the classicality of spatial mode decomposition seems to be common to all SPADE-like approaches. In fact, when SPADE was first introduced [26], it was noted that if the light and photodetection processes are treated using a fully quantum theory, then the classical and quantum Fisher information for the separation estimation problem are equal. It would be interesting to see if this equality is maintained when the classical Fisher information is evaluated in cases where the light is treated classically and the photodetection process semi-classically. This may better inform the community as to whether this technique is truly a quantum solution or merely quantum-inspired.

## 5. Experimental claims of Heisenberg-limited imaging resolution

We know of two instances [7,8] in which experimental studies claimed to demonstrate Heisenberg-limited imaging resolution for extended objects. Both instances relied on the theoretical work of Giovannetti *et al.* [6] to imply that their measured factor of resolution enhancement could not have been achieved using comparable classical illumination.

As was discussed above, the results in [6] establish a Heisenberg-like scaling for the precision with which a Fock state point source can be localized, but it is still unclear whether they yield a definitive quantum advantage for the resolution with which an extended object can be imaged. All that is explicitly shown in [6] is that, in principle, one can use Fock state illumination, photon-number discrimination, and  $N$ -photon detection to construct a quantum imaging system that possesses the resolving characteristics of a coherent imaging system with an effective wavelength of  $\lambda/N$ . What is not shown is that it is impossible for a classical system to achieve the same performance.

Moreover, the existence of an HL for imaging resolution is never referred to in [6]. The authors are much more cautious and simply state that ‘from general principles... one would expect that also a  $1/N$  Heisenberg-like scaling is achievable, i.e., a resolution... not achievable with classical strategies’. Considering the four papers that are cited by the authors of [6] to justify this statement, the general principles that they refer to are presumably single-parameter quantum estimation theory [35,36], a suggestion by Kolobov that multimode squeezed light can be used to improve the resolution of noise-limited (and not diffraction-limited) imaging systems [22], and discussions in a review paper [37] concerning both quantum lithography [5] and a theoretical work by Kolobov & Fabre [38].

Tackling each of these suggestions in turn, we first remind the reader that, as we mentioned in the second section of this paper, imaging an extended object requires (at least) two-dimensional function estimation rather than estimation of a single parameter. Principles that may hold generally across single-parameter estimation strategies may not remain true for function estimation (or even multiparameter estimation). As for the suggestion that multimode squeezed light could improve the resolution of noise-limited imaging systems, this certainly could be true, but it is unrelated to the treatment in [6] in which the presence of noise is not accounted for.

Quantum lithography [5] suffers from the same drawback as the treatment in [6]: it is not proven in [5] that the same enhancement cannot be observed in a classical system, and several works (such as [39], for example) have explicitly suggested otherwise. Finally, the proposal in [38] also does not establish that similar performance could not be achieved using classical methods. Furthermore, it relies on an approach to super-resolution imaging known as bandwidth extrapolation. This approach is known to be extremely susceptible to any non-zero amount of noise and is widely considered to be impractical in a real imaging system (see subsection 8.4.1 of [15], for example).

It is unfortunate that the results of [6] are often interpreted as establishing an SQL and HL for imaging resolution for extended objects. This misunderstanding is perhaps the cause of the experimental claims in [7] and [8] of Heisenberg-limited imaging resolution, claims that appear to be unsupported in the absence of proof that such a limit exists. In particular, we should stress that it is important to verify that the demonstrated spatial resolution of a quantum imaging system is not only superior to that of a single classical system chosen for comparison, but also to that of the best classical system that it could be compared to. The fact that we may not know *a priori* what the best classical system is makes an unambiguous quantum advantage for imaging resolution inherently difficult to demonstrate.

## 6. Conclusion

Quantum metrology and estimation theory can be powerful tools for developing minimally perturbative, high-precision measurement techniques, but only when applied appropriately. In the context of imaging resolution, we have shown that a general purpose technique along these lines remains out of reach for the time being and that if sufficient care is not taken in interpreting results, subtle issues can lead to the appearance of nonclassical performance enhancements in cases where none may actually be present.

To moderate this message, we have shown that while a pre-existing attempt at demonstrating a more general quantum advantage for imaging resolution may have been incomplete, the suggested approach of that study [6] does yield an advantage for two-dimensional point-source localization. This may eventually enable a demonstration of SMLM with super-resolved precision at lower illumination intensities than is possible classically. The realization of this capability, however, will require the development of both fluorophores with Fock state emission and the photon-number-discriminating screen proposed in [6]. Alternatively, the limited near-term feasibility of this approach indicates that a different method for achieving this quantum enhancement would be highly desirable, so perhaps these conclusions will inspire work in that direction.

**Data accessibility.** This article has no additional data.

**Declaration of AI use.** We have not used AI-assisted technologies in creating this article.

**Authors' contributions.** S.I.: conceptualization, formal analysis, investigation, methodology, visualization, writing—original draft, writing—review and editing; Y.X.: formal analysis, methodology, validation, writing—review and editing; R.W.B.: formal analysis, methodology, supervision, validation, writing—review and editing.

All authors gave final approval for publication and agreed to be held accountable for the work performed therein.

**Conflict of interests.** We declare we have no competing interests.

**Funding.** This work was supported by the United States Department of Energy (FWP 76295) and the Natural Sciences and Engineering Research Council of Canada.

**Acknowledgements.** The authors would like to thank James E. Evans for helpful comments made throughout the preparation of this paper.

## References

1. Ganapathy D *et al.* 2023 Broadband quantum enhancement of the LIGO detectors with frequency-dependent squeezing. *Phys. Rev. X* **13**, 041021. (doi:10.1103/PhysRevX.13.041021)
2. Casacio CA, Madsen LS, Terrasson A, Waleed M, Barnscheidt K, Hage B, Taylor MA, Bowen WP. 2021 Quantum-enhanced nonlinear microscopy. *Nature* **594**, 201–206. (doi:10.1038/s41586-021-03528-w)
3. Taylor MA, Bowen WP. 2016 Quantum metrology and its application in biology. *Phys. Rep.* **615**, 1–59. (doi:10.1016/j.physrep.2015.12.002)
4. Santamaria L, Sgobba F, Lupo C. 2024 Single-photon sub-Rayleigh precision measurements of a pair of incoherent sources of unequal intensity. *Opt. Quantum* **2**, 46–56. (doi:10.1364/OPTICAQ.505457)
5. Boto AN, Kok P, Abrams DS, Braunstein SL, Williams CP, Dowling JP. 2000 Quantum interferometric optical lithography: exploiting entanglement to beat the diffraction limit. *Phys. Rev. Lett.* **85**, 2733–2736. (doi:10.1103/PhysRevLett.85.2733)
6. Giovannetti V, Lloyd S, Maccone L, Shapiro JH. 2009 Sub-Rayleigh-diffraction-bound quantum imaging. *Phys. Rev. A* **79**, 013827. (doi:10.1103/PhysRevA.79.013827)
7. Unternährer M, Bessire B, Gasparini L, Perenzoni M, Stefanov A. 2018 Super-resolution quantum imaging at the Heisenberg limit. *Optica* **5**, 1150–1154. (doi:10.1364/OPTICA.5.001150)

8. He Z, Zhang Y, Tong X, Li L, Wang LV. 2023 Quantum microscopy of cells at the Heisenberg limit. *Nat. Commun.* **14**, 2441. (doi:10.1038/s41467-023-38191-4)
9. Kura N, Ueda M. 2020 Standard quantum limit and Heisenberg limit in function estimation. *Phys. Rev. Lett.* **124**, 010507. (doi:10.1103/PhysRevLett.124.010507)
10. Lelek M *et al.* 2021 Single-molecule localization microscopy. *Nat. Rev. Methods Primers* **1**, 39. (doi:10.1038/s43586-021-00038-x)
11. Giovannetti V, Lloyd S, Maccone L. 2011 Advances in quantum metrology. *Nat. Photonics* **5**, 222–229. (doi:10.1038/nphoton.2011.35)
12. Polino E, Valeri M, Spagnolo N, Sciarrino F. 2020 Photonic quantum metrology. *AVS Quantum Sci.* **2**, 2. (doi:10.1116/5.0007577)
13. Boixo S, Flammia ST, Caves CM, Geremia JM. 2007 Generalized limits for single-parameter quantum estimation. *Phys. Rev. Lett.* **98**, 090401. (doi:10.1103/PhysRevLett.98.090401)
14. Demkowicz-Dobrzański R, Kołodyński J, Guţă M. 2012 The elusive Heisenberg limit in quantum-enhanced metrology. *Nat. Commun.* **3**, 1063. (doi:10.1038/ncomms2067)
15. Goodman JW. 2017 *Introduction to fourier optics*. New York, NY: W.H. Freeman, Company.
16. Humphreys PC, Barbieri M, Datta A, Walmsley IA. 2013 Quantum enhanced multiple phase estimation. *Phys. Rev. Lett.* **111**, 070403. (doi:10.1103/PhysRevLett.111.070403)
17. Górecki W, Demkowicz-Dobrzański R. 2022 Multiple-phase quantum interferometry: real and apparent gains of measuring all the phases simultaneously. *Phys. Rev. Lett.* **128**, 040504. (doi:10.1103/PhysRevLett.128.040504)
18. Morris PA, Aspden RS, Bell JEC, Boyd RW, Padgett MJ. 2015 Imaging with a small number of photons. *Nat. Commun.* **6**, 5913. (doi:10.1038/ncomms6913)
19. Zhang B, Zerubia J, Olivo-Marin JC. 2007 Gaussian approximations of fluorescence microscope point-spread function models. *Appl. Opt.* **46**, 1819–1829. (doi:10.1364/ao.46.001819)
20. Tsang M. 2015 Quantum limits to optical point-source localization. *Optica* **2**, 646–653. (doi:10.1364/OPTICA.2.000646)
21. Genovese M. 2016 Real applications of quantum imaging. *J. Opt.* **18**, 073002. (doi:10.1088/2040-8978/18/7/073002)
22. Kolobov MI. 1999 The spatial behavior of nonclassical light. *Rev. Mod. Phys.* **71**, 1539–1589. (doi:10.1103/RevModPhys.71.1539)
23. Wolley O, Gregory T, Beer S, Higuchi T, Padgett M. 2022 Quantum imaging with a photon counting camera. *Sci. Rep.* **12**, 8286. (doi:10.1038/s41598-022-10037-x)
24. Ourjoumtsev A, Tualle-Brouiri R, Grangier P. 2006 Quantum homodyne tomography of a two-photon fock state. *Phys. Rev. Lett.* **96**, 213601. (doi:10.1103/PhysRevLett.96.213601)
25. Cooper M, Wright LJ, Söller C, Smith BJ. 2013 Experimental generation of multi-photon fock states. *Opt. Express* **21**, 5309–5317. (doi:10.1364/OE.21.005309)
26. Tsang M, Nair R, Lu XM. 2016 Quantum theory of superresolution for two incoherent optical point sources. *Phys. Rev. X* **6**, 031033. (doi:10.1103/PhysRevX.6.031033)
27. Paúr M, Stoklasa B, Hradil Z, Sánchez-Soto LL, Rehacek J. 2016 Achieving the ultimate optical resolution. *Optica* **3**, 1144–1147. (doi:10.1364/OPTICA.3.001144)
28. Horstmeyer R, Heintzmann R, Popescu G, Waller L, Yang C. 2016 Standardizing the resolution claims for coherent microscopy. *Nat. Photonics* **10**, 68–71. (doi:10.1038/nphoton.2015.279)
29. Goodman JW. 2015 *Statistical optics*. Hoboken, NJ: John Wiley & Sons.
30. Betzig E. 2015 Nobel lecture: single molecules, cells, and super-resolution optics. *Rev. Mod. Phys.* **87**, 1153–1168. (doi:10.1103/RevModPhys.87.1153)
31. Hell SW. 2015 Nobel lecture: nanoscopy with freely propagating light. *Rev. Mod. Phys.* **87**, 1169–1181. (doi:10.1103/RevModPhys.87.1169)
32. Moerner WE. 2015 Nobel lecture: single-molecule spectroscopy, imaging, and photocontrol: foundations for super-resolution microscopy. *Rev. Mod. Phys.* **87**, 1183–1212. (doi:10.1103/RevModPhys.87.1183)
33. Deshler N, Haffert S, Ashok A. 2024 Achieving quantum limits of exoplanet detection and localization. *arXiv* (doi:arXiv:240317988)
34. Kupianskyi H, Horsley SAR, Phillips DB. 2023 High-dimensional spatial mode sorting and optical circuit design using multi-plane light conversion. *APL. Photon* **8**, 026101. (doi:10.1063/5.0128431)

35. Giovannetti V, Lloyd S, Maccone L. 2006 Quantum metrology. *Phys. Rev. Lett.* **96**, 010401. (doi:10.1103/PhysRevLett.96.010401)
36. Braunstein SL. 2006 Size isn't everything. *Nature* **440**, 617–618. (doi:10.1038/440617a)
37. Giovannetti V, Lloyd S, Maccone L. 2004 Quantum-enhanced measurements: beating the standard quantum limit. *Science* **306**, 1330–1336. (doi:10.1126/science.1104149)
38. Kolobov MI, Fabre C. 2000 Quantum limits on optical resolution. *Phys. Rev. Lett.* **85**, 3789–3792. (doi:10.1103/PhysRevLett.85.3789)
39. Hemmer PR, Muthukrishnan A, Scully MO, Zubairy MS. 2006 Quantum lithography with classical light. *Phys. Rev. Lett.* **96**, 163603. (doi:10.1103/PhysRevLett.96.163603)